Desalination and Water Treatment
www.deswater.com

doi: 10.1080/19443994.2014.976276

57 (2016) 1693–1704
January

Preparation and evaluation of chitosan-coated eggshell particles as copper(II) biosorbent

Jafar Mohammadnezhad[a,*], Fardin Khodabakhshi-Soreshjani[b], Hadi Bakhshi[c]

[a]*Department of Chemistry, Shahr-e-Qods Branch, Islamic Azad University, Tehran, Iran, Tel. +98 21 46896000; Fax: +98 21 46896519; email: behkia3316@yahoo.com*
[b]*Department of Chemistry, Karaj Branch, Islamic Azad University, Karaj, Iran, Tel. +98 21 48662121; email: fardin3154@yahoo.com*
[c]*Department of Chemical and Petroleum Engineering, Sharif University of Technology, P.O. Box: 11365-11155, Tehran, Iran, Tel. +98 21 66166452; emails: hadibakhshi@yahoo.com, hbakhshi@che.sharif.edu*

Received 16 June 2014; Accepted 5 October 2014

ABSTRACT

Preparation and evaluation of chitosan-coated eggshell (CTS-ES) particles as a biosorbent for removal of Cu(II) ions from aqueous media was considered in this research. For this purpose, chitosan was coated on eggshell (ES) particles through precipitation procedure. The coated particles were characterized by Fourier transform infrared, thermogravimetric analysis, and field emission scanning electron microscopy analysis. Kinetic studies showed that coating of chitosan on ES particles improved their Cu(II) adsorption capacity. The removal of Cu(II) ions by either ES or CTS-ES particles followed the pseudo-second-order kinetics, indicating that chemical sorption is the rate-limiting step for both of them. Langmuir and Freundlich models were used to describe the mechanism of the Cu(II) adsorption. The data fitted well with the Langmuir model, showing both ES and CTS-ES particles are homogenous adsorbents. The coated particles had maximum Cu(II) adsorption capacity of 95.2 mg/g, which was higher than that of ES particles (73.5 mg/g). The adsorption capacities of the either ES or CTS-ES particles were reduced with decreasing the pH and ionic strength of media. Therefore, the prepared CTS-ES particles can be used as a potential renewable resource-based and cost-effective biosorbent for removal of Cu(II) ions from aqueous media.

Keywords: Chitosan; Eggshell particles; Cu(II) removal; Kinetics; Isotherms

---

1. Introduction

The increasing level of toxic heavy metal ions discharged to the environment is currently an important concern, as a result of their adverse effects on either public health or ecological systems [1]. Mining activities, metal fabrication, electroplating, battery manufacturing, and illegal landfills are potential sources of heavy metal ions [1,2]. Furthermore, natural weathering processes, atmospheric depositions, and anthropogenic activities are other reasons for the contamination of water to these ions [2]. Although copper is one of essential elements to human body in trace quantities, high levels of Cu(II) ions are toxic and may cause various health problems in liver, kidney, and

---

*Corresponding author.

central nervous system [3]. High concentrations of Cu(II) ions can also cause cancer and promote oxidation in body [4]. Furthermore, Cu(II) ions are toxic to aquatic organisms like fishes at low pH values [5]. Therefore, it is important to remove any excess amount of Cu(II) ions present in wastewater; so that it can prevent the contamination of the surface water and ground water, and protect the public health.

Wastewater contaminated with heavy metal ions can be treated by various methods such as chemical precipitation, ion-exchange, adsorption, membrane filtration, coagulation–flocculation, flotation, and electrochemical processes [6]. In particular, adsorption method is recognized as a relatively simple and effective one [6].

Recently, remarkable activities have been observed for the development of low-cost adsorbents based on waste materials [7]. Eggshell (ES) constitutes ~10% of the total mass of hen egg (~60 g) [8] and is composed by calcium carbonate (94%), calcium phosphate (1%), magnesium carbonate (1%), and organic matter (4%) [8]. A huge amount of ES is produced daily by food manufacturers and restaurants, which are basically of no use causing environmental pollution. Many investigations have shown that ES particles are able to adsorb metal ions [9–11], dyestuffs [12,13] and organic compounds [14].

Using renewable resource-based materials such as biopolymers for the environmental clean-up have also attracted growing interests during last two decades [15]. Due to biodegradability, inexpensiveness, and great availability, they are competitive with ion-exchange resins and activated carbon. Chitosan is an alkaline deacetylation product of chitin founding in crustaceous shells, insects, and fungal cell walls [16,17]. Chitosan contains high content of amine and hydroxyl groups, which are favorable for the complexation with metal ions [5,18,19], thus has the highest adsorption capacity among the biopolymers [2,20]. The key technical issues for the application of chitosan as a biosorbent are poor mechanical properties (softness) and dissolvation in dilute acidic media (forming a gel) [21]. To overcome these drawbacks, chitosan can be cross-linked [1,20,22] or immobilized on supporting materials such as alumina [21,23], bentonite [3,15,24–26], glass beads [27], perlite [28–31], PVC beads [32], and sand [2,33,34]. Coating chitosan on supports also results in lower amounts of chitosan being used, and thus lowers the cost of the final adsorbent. Therefore, the aim of this study is the coating of chitosan on ES particles as waste material, to result in a renewable resource-based and low-cost biosorbent with overall adsorption capacity of pure chitosan.

In this study, chitosan was coated on ES particles through precipitation procedure to prepare biosorbent for removal of Cu(II) ions from aqueous media. The chemical structure, size and surface morphology of the particles were studied by instrumental analysis. The potency of the particles for Cu(II) adsorption from aqueous media was evaluated under various experimental conditions to demonstrate adsorption kinetics, isotherms, pH, and ionic strength effects.

2. Experimental

2.1. Materials

Hen ESs were collected from a local restaurant in Tehran. Chitosan was supplied by Bechmann-Kenko and used as received. Oxalic acid dihydrate ($(COOH)_2 \cdot 2H_2O$), sodium hydroxide (NaOH), copper dinitrate trihydrate ($Cu(NO_3)_2 \cdot 3H_2O$), sodium nitrate ($NaNO_3$), and acetone were bought from Merck.

2.2. Preparation of ES particle

Collected ES was washed with hot distilled water to remove the impurities. The cleaned ES was dried at 70°C in a hot air oven for 4 h. The dried ES, without membrane separation, was grounded into powder using a grinder and then sieved into size ranges of 100–200 mesh (75–150 μm).

2.3. Preparation of chitosan-coated ES particles

Chitosan was coated on ES particles through precipitation procedure. In a 250 mL beaker, 1 g of chitosan was added to 100 mL oxalic acid solution (0.2 M) and magnetically stirred at 750–1,000 rpm for 30 min in order to complete dissolvation. Then, 5 g of ES particles was added to the solution and stirred for 5 min. After that sodium hydroxide solution (1 M) was added dropwise to the stirring mixture until its pH increased up to 7. The mixture was further stirred for 15 min and then centrifuged at 1,000 rpm for 1 min to sediment chitosan-coated eggshell (CTS-ES) particles. The separated particles were kept in 100 mL of acetone for 1 h in order to complete dehydration. Finally, the coated particles were dried at 40°C in a vacuum oven for 6 h and stored away from moisture before use.

2.4. Instruments

The Fourier transform infrared (FTIR) spectroscopy was accomplished using a Bruker spectrophotometer (model Equinox 55, Germany) in the range of 400–4,000 cm^{-1} at 4 cm^{-1} resolution and 16 scans. Thermogravimetric analysis (TGA) was carried out on a Mettler-Toledo instrument (model TGA/DSC 1, Switzerland) from 25 to 600°C at a heat rate of 10°C/min under nitrogen atmosphere. Size and surface morphology of the particles were evaluated using field emission scanning electron microscopy (FE-SEM, model Mira, Tescan, Czech). The particles were fixed on an aluminum pin using double-sided adhesive tape and then sputter coated with a thin gold layer for 4 min before microscopy. UV–visible spectrometry was carried out using a Biochrom spectrophotometer (model WPA S2000 Lightwave, UK) at ambient temperature. Distilled water was used as blank medium.

2.5. Adsorption experiments

Investigation of Cu(II) adsorption onto the particles was carried out in batch experiments. For this purpose, 50 mg of the particles was placed into 25 mL vials containing 10 mL aqueous solution with desired concentrations of Cu(II) ions (50–800 mg/L), pH values (2–5) and sodium nitrate (0–20 g/L). The mixtures were shaken by a rotary shaker at 25°C and 150 rpm for 0.5–8 h. After desired intervals, the vials were centrifuged at 4,000 rpm for 1 min to precipitate the particles. Then, the aqueous media were filtered using a filter paper and the concentrations of remained Cu(II) ions in the media were determined using UV–visible spectrometry. Cu(II) adsorption capacity (q, mg/g) and removal efficiency (RE, %) were calculated using the following equations:

$$q = \frac{(C_0 - C_t)V}{m} \tag{1}$$

$$\mathrm{RE} = \frac{(C_0 - C_t)}{C_0} \times 100 \tag{2}$$

where C_0 (mg/L) and C_t (mg/L) are, respectively, the initial Cu(II) concentrations in the solution and after contacting with the particles for time t (min), V (L) is the volume of solution, and m (g) is the mass of the particles.

UV–visible spectrometry was carried out at 250 nm. The concentrations of Cu(II) ions in aqueous media were calculated using a seven-point calibration curve in the range of 1–1,000 mg/L. The reported values are an average of three measurements.

3. Results and discussion

3.1. Characterization of the particles

Chitosan was coated on ES particles through precipitation procedure to prepare biosorbent for removal of Cu(II) from aqueous media. Chitosan is soluble in acidic media and solidifies in neutral and alkaline media. This phenomenon offers its precipitation on the surface of ES particles through increasing the pH of media.

The chemical structures of the raw materials and coated particles were studied through FTIR spectroscopy. FTIR spectra of ES particles, chitosan, and CTS-ES particles are depicted in Fig. 1. FTIR spectrum of ES particles (Fig. 1(a)) showed the typical peaks of calcium carbonate (2,516, 1,798, 1,418, 875, and 712 cm^{-1}) as main component of ES. The peaks at 1,418, 875, and 712 cm^{-1} are related to asymmetric stretching (ν3), and in-plane and out-of-plane bending vibrations of carbonate moiety, respectively [35,36]. FTIR spectrum of chitosan (Fig. 1(b)) confirmed the presence of saturated hydrocarbons in its backbone. The stretching vibrations of O–H and N–H bonds of hydroxyl and amine groups, respectively, appeared as

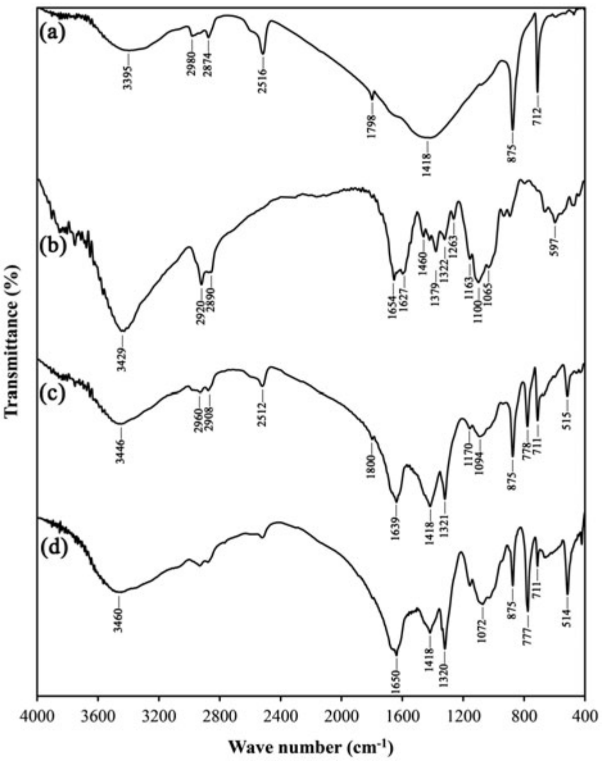

Fig. 1. FTIR spectra of ES particles (a), chitosan (b), CTS-ES particles before (c) and after (d), and adsorption of Cu(II) ions.

a wide peak centered at 3,429 cm^{-1} [21,23,37]. The peaks at 2,920 and 2,890 cm^{-1} are attributed to stretching vibration of aliphatic C–H bonds [21,23,37]. The bending vibrations of N–H bonds of amine groups were also observed at 1,654 and 1,627 cm^{-1} [21,23]. The peaks at 1,460 and 1,379 cm^{-1} belong to bending vibrations of $–CH_2–$ and $–CH_3$ groups, respectively [37]. The stretching vibration of C–N bonds of amine groups appeared at 1,263 cm^{-1}. The peak at 1,163 cm^{-1} is due to asymmetric stretching vibration of C–O bonds of ether bridges, while the skeletal stretching vibration of C–O bond of hydroxyl groups was observed at 1,065 cm^{-1} [21,23]. These two peaks are generally considered as the fingerprint peaks for the polysaccharide structure of chitosan [37,38]. The occurrence of corresponding peaks for ES (2,512, 1,800, 1,418, 875, and 711 cm^{-1}) and chitosan (1,639, 1,321, 1,170, and 1,094 cm^{-1}) in the FTIR spectrum of CTS-ES particles (Fig. 1(c)) confirmed their combination within the coated particles. Meanwhile, this reveals that adsorption sites of chitosan (amine and hydroxyl groups) remained intact during coating on ES particles and are available for the complexation with Cu(II) ions.

The FTIR spectrum of CTS-ES particles after adsorption of Cu(II) ions (Fig. 1(d)) indicated a shift for peak belongs to stretching vibration of O–H and N–H bonds of hydroxyl and amine groups, respectively, to higher wave number values (from 3,446 to 3,460 cm^{-1}). The peak related to bending vibration of N–H bonds of amine groups also shifted to higher wave number values (from 1,639 to 1,650 cm^{-1}). This phenomenon is in agreement with previous reports [29,31,39] and is due to deformation of O–H and N–H bonds of hydroxyl and amine groups, respectively, as a result of interaction between with Cu(II) ions.

The weight percent of chitosan in the coated particles was determined by means of TGA [25]. TGA and DTGA curves of ES particles, chitosan, and CTS-ES particles are presented in Fig. 2. ES particles were thermally stable up on 600℃ with a weight loss of 3.7% relating to volatile materials [40]. TGA and DTGA curves of chitosan reveal two stages of mass loss. The first mass loss stage at temperature region of 50–100℃ (weight loss 7.6%) is due to the loss of physically adsorbed water. The second mass loss stage (weight loss 40.4%) at temperature region of 250–330℃ is related to degradation of hydrocarbons within chitosan backbone [1,2,25]. The ash content of chitosan at 600℃ was 32.4%. TGA and DTGA curves of CTS-ES particles show multiple stages of weight loss similar to that of chitosan. The ash content of the coated particles at 600℃ was 84.4%. According to the ash content values, the weight percent of chitosan in the coated particles was calculated as 18.6% (theoretical value was 16.7%). The difference between experimental and theoretical values can be attributed to measurement errors of DTA analysis and agglomeration of the chitosan chains to form some chitosan particles instead of coating on the ES particles, which led in higher chitosan within the sample for TGA analysis.

The size and surface morphology of the particles were studied through FE-SEM. FE-SEM images of ES particles, chitosan, and CTS-ES particles are shown in Fig. 3. FE-SEM images ES particles (Fig. 3(a) and (b)) exhibit a particle size range of 100–200 μm and angular pattern of fractures due to their crystalline structure [35] with rough and irregular surfaces. The fibers of ES membrane were clearly observed on surface of ES particles. For better comparison, chitosan was also dissolved in oxalic acid solution (0.2 M) and precipitated through dropwise addition of sodium hydroxide solution (1 M) under magnetic stirring. FE-SEM image of chitosan (Fig. 3(c) and (d)) shows a porous structure. FE-SEM image of the coated particles (Fig. 3(e) and (f)) displays particle size range similar to ES particles (100–200 μm), while their surfaces were covered with chitosan and no evidence of the ES membrane fibers was observed. The adsorption sites belong to immobilized chitosan chains (amine and hydroxyl groups) will improve the Cu(II) adsorption capacity of the coated particles comparing to ES particles.

3.2. Kinetics of Cu(II) adsorption onto the particles

The adsorption kinetics of Cu(II) ions onto the particles are depicted in Fig. 4. According to Fig. 4, 96.3% of Cu(II) ions were removed by CTS-ES particles within the first 2 h, while the removal efficiency for ES particles was gradually increased to 69.3% within 7 h. The equilibrium adsorption capacities (q_e) of ES and CTS-ES particles were 13.9 ± 0.4 and 19.6 ± 0.6 mg/g, respectively. The different adsorption kinetics of these particles is due to diverse adsorption sites on their surfaces. Adsorption and precipitation are two mechanisms for removal of Cu(II) ions by ES particles, while both involve reactions with the surface of $CaCO_3$ in the ES particles [10,41]. Adsorption occurs at low Cu(II) concentrations through complexation with carbonyl bonds of carbonate groups. Precipitation happens at high Cu(II) concentrations via ion-exchange with Ca^{2+} ions [10,41]. For the coated particles, amine and hydroxyl groups of chitosan adsorb the Cu(II) ions through formation of stable complexes [5,18,19]. These adsorption sites are readily accessible from outer interface, and thus resulted in rapid adsorption process.

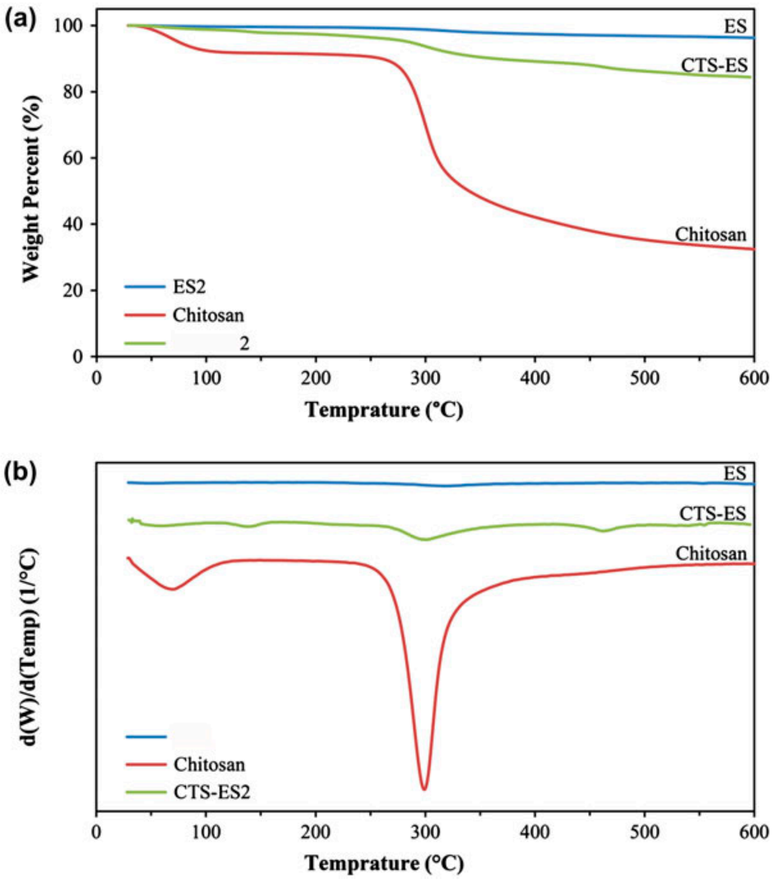

Fig. 2. TGA (a) and DTGA (b) curves for ES particles, chitosan, and CTS-ES particles.

In order to investigate the kinetic mechanism of the Cu(II) adsorption by ES and CTS-ES particles, the experimental data were analyzed according to the linear forms of the pseudo-first-order (PFO) and pseudo-second-order (PSO) kinetic models. The linear forms of the PFO and PSO models can be expressed according to following equations [42,43]:

$$\ln(q_e - q_t) = \ln q_e - k_1 t \tag{3}$$

$$\frac{t}{q_t} = \frac{t}{q_e} + \frac{1}{k_2 q_e^2} \tag{4}$$

where q_t (mg/g) is the amount of adsorbed Cu(II) at time t (min), and k_1 (1/min) and k_2 (g/mg min) are, respectively, the rate constants of PFO and PSO adsorptions. For PFO model, the values of k_1 and q_e were obtained from the slope and intercept of ln $(q_e - q_t)$ vs. t plot, respectively. For PSO model, the slope and intercept of t/q_t vs. t plot showed, respectively, q_e and k_2 values.

The results for the kinetic parameters are given in Table 1. The regression correlation coefficient (R^2) values were reported to indicate the goodness of the kinetic model fit. For either ES or CTS-ES particles, higher R^2 values were obtained with the PSO model compared to the PFO model (Table 1). Moreover, the calculated equilibrium adsorption capacities ($q_{e\text{-cal}}$) obtained from the PSO model were well approximated to the experimental ones, especially for CTS-ES particles, indicating better suitability of this model to describe Cu(II) adsorption kinetics onto these particles. Chemisorption is the rate-controlling step for the overall sorption processes following PSO kinetics [2,18,44]. This is in agreement with Cu(II) adsorption onto the chitosan chains involving complexation of their amine and hydroxyl groups with Cu(II) ions [5,18,19]. Several studies showed that the adsorption of Cu(II) ions onto chitosan and supported chitosan followed the PSO kinetics [3,18,24,25].

As expected, the k_2 value was higher for CTS-ES particles (8.60×10^{-3} g/mg min) in comparison to ES particles (5.52×10^{-4} g/mg min) due to presence of

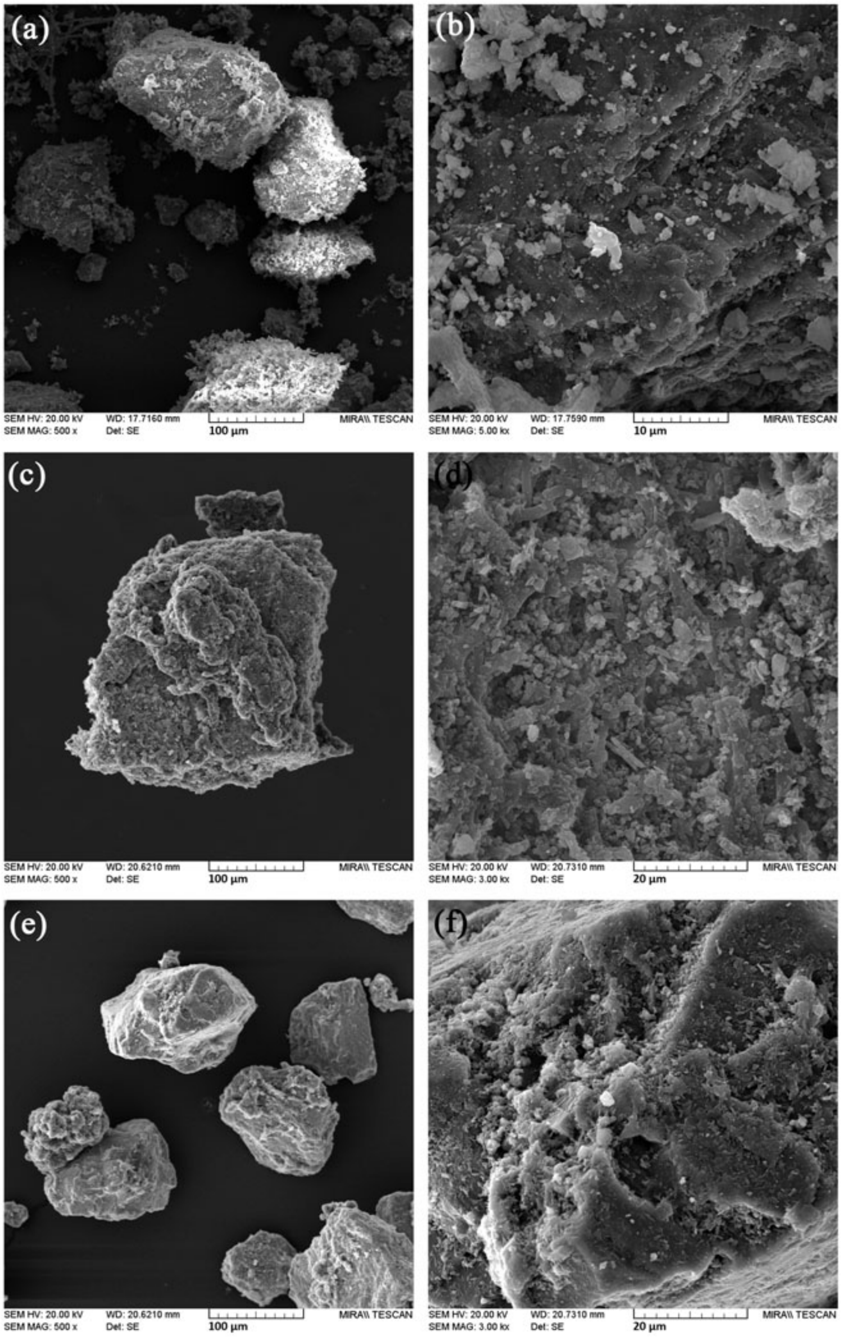

Fig. 3. SEM images of ES particles (a, b), chitosan (c, d), and CTS-ES (e, f) particles.

amine and hydroxyl groups of chitosan with high adsorbability for Cu(II) ions [5,18,19].

3.3. Isotherms of Cu(II) adsorption onto the particles

Adsorption isotherms describe the distribution of Cu(II) ions between the surface of the particles and aqueous medium at equilibrium [45]. The q_e values for the particles vs. equilibrium concentrations of Cu(II) in aqueous media (C_e) are depicted in Fig. 5. For both ES and CTS-ES particles, q_e values were progressively increased with C_e ones reaching the saturation of the particles.

The Langmuir and Freundlich isotherm models were used to determine maximum Cu(II) adsorption capacities of the particles. The Langmuir model has

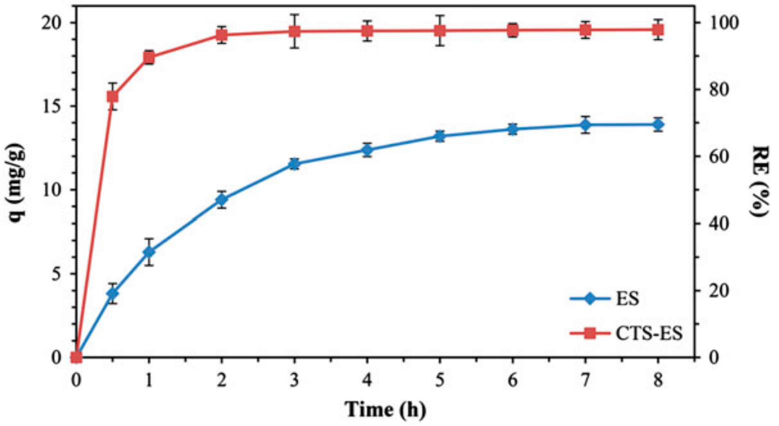

Fig. 4. Cu(II) adsorption kinetics for the particles. Initial Cu(II) concentration: 100 mg/L, particles dose: 5 g/L, pH 5, and 25°C.

Table 1
Kinetic parameters for Cu(II) adsorption by the particles[a]

		PFO kinetic model			PSO kinetics model		
Particles	q_e (mg/g)	k_1 (1/min)	$q_{e\text{-cal}}$ (mg/g)	R^2	k_2 (g/mg min)	$q_{e\text{-cal}}$ (mg/g)	R^2
ES	13.9 ± 0.4	1.38×10^{-2}	23.1	0.886	5.52×10^{-4}	17.5	0.998
CTS-ES	19.6 ± 0.6	1.24×10^{-2}	2.48×10^{-1}	0.893	8.60×10^{-3}	19.9	0.999

[a] All experiments were performed at initial Cu(II) concentration: 100 mg/L, particles dose: 5 g/L, pH 5, and 25°C.

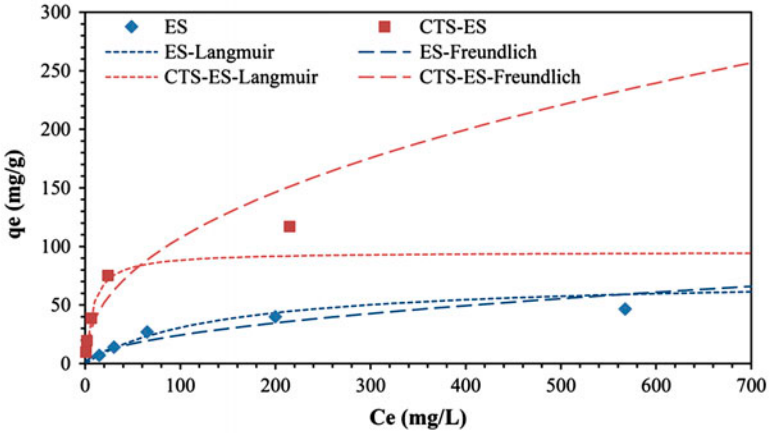

Fig. 5. Cu(II) adsorption isotherms for the particles. Particles dose: 5 g/L, pH 5, contact time: 8 h, and 25°C.

been commonly used for studying the adsorption in solution and assumes that Cu(II) adsorption occurs at specific homogeneous sites with equal adsorption energy [1]. The linear form of this model is expressed as follows [1]:

$$\frac{1}{q_e} = \frac{1}{q_m K_L C_e} + \frac{1}{q_m} \tag{5}$$

where q_m (mg/g) is the Langmuir adsorption capacity representing the maximum adsorption capacity of the monolayer formed on the particles and K_L (L/mg) is the Langmuir constant related to enthalpy of adsorption. K_L is a measure of affinity of the adsorbate for the adsorbent [46]. The values of q_m and K_L were obtained from the intercept and slope of the $1/q_e$ vs. $1/C_e$ plot, respectively. Furthermore, the separation factor or the equilibrium parameter (R_L) was calculated according to the following equation [47]:

$$R_L = \frac{1}{1 + K_L C_0} \tag{6}$$

The R_L value indicates whether the adsorption is unfavorable ($R_L > 1$), linear ($R_L = 1$), favorable ($0 < R_L < 1$), or irreversible ($R_L = 0$).

The Freundlich model has also been used to describe the adsorption equilibrium. This model is an empirical equation employed to describe equilibrium on heterogeneous surfaces, and hence does not assume monolayer capacity [1]. The linear logarithmic form of the Freundlich model can be written as follows:

$$\ln q_e = \ln K_F + \frac{1}{n} \ln C_e \tag{7}$$

where K_F (L/g) and n are the Freundlich constants relating to the adsorption capacity and adsorption intensity, respectively. The values of K_F and n were, respectively, obtained from the intercept and slope of the ln q_e vs. ln C_e plot. The obtained value of $n > 1$ indicates favorable adsorption conditions [44].

The Langmuir and Freundlich isotherms for Cu(II) adsorption onto the particles are given in Table 2. For either ES or CTS-ES particles, the R_L and n values were in the range of $0 < R_L < 1$ and $n > 1$, respectively, which show that Cu(II) adsorption onto these particles was favorable processes [48]. According to the R^2 values, for both ES and CTS-ES particles, the Langmuir model provided better fit for the experimental data in comparison to the Freundlich model. FTIR and isotherms results are in agreement with previous reports, which claimed that adsorption of Cu(II) ions on chitosan and supported chitosan occurred trough complexation with amine and hydroxyl groups and followed Langmuir isotherms [21,29,31,32,39]. Since Langmuir isotherm refers to homogenous adsorption process [1], it may be concluded that amine and hydroxyl groups of chitosan have similar energy level as binding sites for Cu(II) ions. It can also concluded that chitosan chains completely covered the surface of ES particles during coating procedure.

The Langmuir model was used to interpret the adsorption of Cu(II) ions onto these particles. The coated particles had maximum Cu(II) adsorption capacity of 95.2 mg/g, which was higher than that of ES particles (73.5 mg/g). Furthermore, higher K_L and lower R_L values for CTS-ES particles comparing to ES particles, confirmed that the coated particles have higher affinity to adsorb Cu(II) ions [49–51].

The maximum Cu(II) adsorption capacities (q_m) provided by Langmuir isotherm are compared with those for other adsorbents based on ES and chitosan in Table 3. The CTS-ES particles developed in the present study exhibits higher adsorption capacity compared to most of chitosan-coated supports.

3.4. Effect of pH on Cu(II) adsorption onto the particles

The pH of the media is an important parameter in adsorption processes. The effect of pH of solution on Cu(II) adsorption by the particles in the pH range of 2–5 is shown in Fig. 6. This pH range was chosen, since chitosan undergoes dissolvation below pH 2 and copper ions precipitate above pH 5 [31]. For either ES or CTS-ES particles, the Cu(II) adsorption capacities were reduced as the pH of medium decreased. Similar trend was observed for Cu(II) adsorption by chitosan [22,52] and immobilized chitosan [2,3,32]. The lower Cu(II) adsorption capacity of CTS-ES particles at acidic pH values can be attributed to three reasons: (1) protonation of amine and hydroxyl groups within chitosan backbone and their consequent electrostatic repulsion with Cu(II) ions [2,21,53], (2) competition between (H_3O^+) hydronium ions and Cu(II) ions in terms of binding with adsorption sites [1,21], and (3) dissolvation of chitosan in acidic media. The competition reactions can be written as follows:

Table 2
Langmuir and Freundlich isotherms for Cu(II) adsorption by the particles[a]

	Langmuir isotherm model				Freundlich isotherm model		
Particles	q_m (mg/g)	K_L (L/mg)	R^2	R_L	K_F (L/g)	n	R^2
ES	73.5	7.18×10^{-3}	0.992	0.148–0.736	2.29	1.95	0.890
CTS-ES	95.2	1.26×10^{-1}	0.997	0.010–0.137	13.6	2.23	0.939

[a] All experiments were performed at particles dose: 5 g/L, pH 5, contact time: 8 h, and 25°C.

Table 3
Cu(II) adsorption capacities of various adsorbents based on ES particles and chitosan

Adsorbent	pH	Maximum Cu(II) adsorption capacity (q_m, mg/g)	Kinetic model	Isotherm	Reference
Chitosan beads	6	80.7		Langmuir	[22]
Chitosan coated ceramic alumina	4	86.2		Langmuir	[21]
Chitosan coated activated alumina	6	315.5		Langmuir	[23]
Chitosan coated bentonite	4	12.2	PSO	Langmuir	[3]
Chitosan coated bentonite	4	18.8	PSO	Freundlich	[25]
Chitosan coated bentonite	4	12.6	PSO	Freundlich	[24]
Chitosan coated bentonite and crosslinked with epichlorohydrin	4	9.4	PSO	Freundlich	[22]
Chitosan coated perlite	5	196.1	PSO	Langmuir	[31]
Chitosan coated perlite	4.5	104.0		Langmuir	[30]
Chitosan coated PVC beads	4	87.9	SO	Langmuir	[32]
Chitosan coated sand	4.2	10.9		Langmuir	[33]
Chitosan coated sand	4.5	8.2	PSO	Langmuir	[2]
ES particles	5.5	32.3		Langmuir	[10]
ES particles		51.7	PSO	Langmuir	[56]
ES particles	5	73.5	PSO	Langmuir	This work
Chitosan coated ES particles	5	95.2	PSO	Langmuir	This work

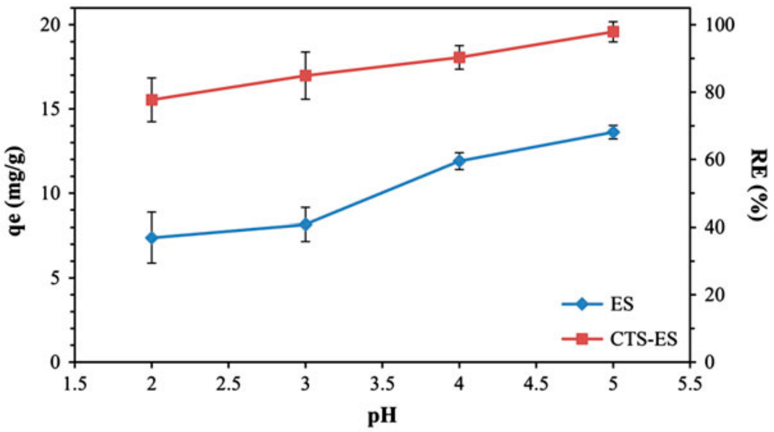

Fig. 6. Effect of pH on Cu(II) adsorption by the particle. Initial Cu(II) concentration: 100 mg/L, particles dose: 5 g/L, contact time: 8 h, and 25˚C.

$$\mathrm{CTS-NH_2+Cu^{2+}\rightarrow(CTS-NH_2)^{2+}Cu} \quad (8)$$

$$\mathrm{CTS-NH_2+H^{+}\rightarrow CTS-NH_3^{+}} \quad (9)$$

At higher pH values, more adsorption sites of chitosan (amine and hydroxyl groups) have a negative charge, which promote their interaction with the Cu(II) ions [32,54].

3.5. Effect of ionic strength on Cu(II) adsorption onto the particles

Ionic strength of the media is an important parameter in adsorption process, especially when adsorbate removal is affected by slight changes in the supporting electrolyte solution [55]. To study the effect of ionic strength of media on Cu(II) adsorption by the particles, Cu(II) solutions contain different amounts of $NaNO_3$ (0–20 g/L) were used. The result is displayed

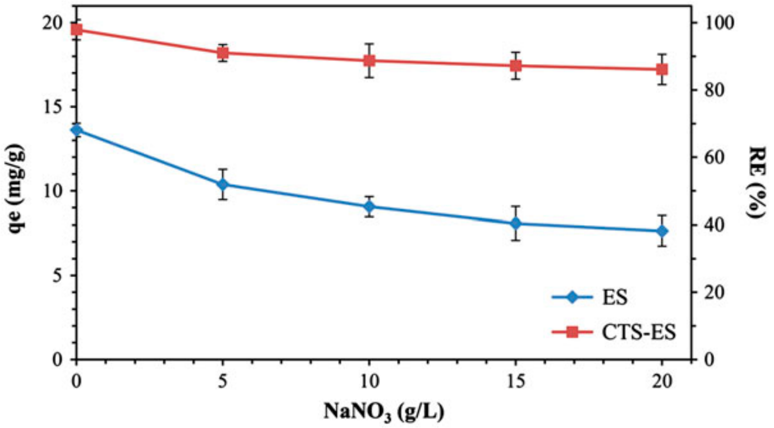

Fig. 7. Effect of ionic strength on Cu(II) adsorption by the particle. Initial Cu(II) concentration: 100 mg/L, particles dose: 5 g/L, contact time: 8 h, and 25℃.

in Fig. 7. For either ES or CTS-ES particles, the Cu(II) adsorption capacities were reduced as the concentration of $NaNO_3$ and consequently ionic strength of the medium increased. Similar trend was observed for the Cu(II) adsorption by chitosan [55] and immobilized chitosan [24]. Upon addition of $NaNO_3$, the Na^+ ions distribute the outer layer surrounding the particles, providing strong repulsive forces to the Cu(II) ions and lead to a decrease in the adsorption capacity of the particles [24].

Increasing the concentration of $NaNO_3$ from 0 to 20 g/L caused a minimal reduction in Cu(II) adsorption of CTS-ES particles (from 97.9% to 86.1%) comparing to ES particles (from 68.1% to 38.2%). In fact, chitosan chains do not form complexes with Na^+ ions [24], which implies that increasing their concentration has insignificant effect on the adsorption of Cu(II) ions on the coated particles.

4. Conclusions

Chitosan was successfully coated on the surface of ES particles through precipitation procedure. The coated particles were characterized by FTIR, TGA, and FE-SEM analysis. Coating of chitosan on ES particles improved their Cu(II) adsorption capacity from 13.9 ± 0.4 to 19.6 ± 0.6 mg/g. The removal of Cu(II) ions by either ES or CTS-ES particles followed the pseudo-second-order kinetics, indicating that chemical sorption is the rate-limiting step for both of them. The k_2 value was higher for CTS-ES particles in comparison to ES particles due to presence of amine and hydroxyl groups of chitosan with high adsorbability for Cu(II) ions. The data fitted well with the Langmuir model, showing both ES and CTS-ES particles are homogenous adsorbents. The coated particles had maximum Cu(II) adsorption capacity of 95.2 mg/g, which was higher than that of ES particles (73.5 mg/g). Furthermore, the K_L and lower R_L values for CTS-ES particles were high comparing to ES particles. For either ES or CTS-ES particles, the Cu(II) adsorption capacities were reduced with decreasing the pH and ionic strength of media. These results demonstrated the potential utility of the CTS-ES particles for removal of Cu(II) ions from aqueous media.

References

[1] R. Laus, T.G. Costa, B. Szpoganicz, V.T. Fávere, Adsorption and desorption of Cu(II), Cd(II) and Pb(II) ions using chitosan crosslinked with epichlorohydrin-triphosphate as the adsorbent, J. Hazard. Mater. 183 (2010) 233–241.

[2] M.W. Wan, C.C. Kan, B.D. Rogel, M.L.P. Dalida, Adsorption of copper(II) and lead(II) ions from aqueous solution on chitosan-coated sand, Carbohydr. Polym. 80 (2010) 891–899.

[3] M.L.P. Dalida, A.F.V. Mariano, C.M. Futalan, C.-C. Kan, W.-C. Tsai, M.-W. Wan, Adsorptive removal of Cu(II) from aqueous solutions using non-crosslinked and crosslinked chitosan-coated bentonite beads, Desalination 275 (2011) 154–159.

[4] R. Schmuhl, H.M. Krieg, K. Keizer, Adsorption of Cu (II) and Cr(IV) ions by chitosan: Kinetics and equilibrium studies, Water SA 27 (2001) 1–7.

[5] W.S.W. Ngah, S. Fatinathan, Adsorption of Cu(II) ions in aqueous solution using chitosan beads, chitosan-GLA beads and chitosan-alginate beads, Chem. Eng. J. 143 (2008) 62–72.

[6] F. Fu, Q. Wang, Removal of heavy metal ions from wastewaters: A review, J. Environ. Manage. 92 (2011) 407–418.

[7] J. Carvalho, J. Araujo, F. Castro, Alternative low-cost adsorbent for water and wastewater decontamination derived from eggshell waste: An overview, Waste Biomass Valorization 2 (2011) 157–167.

[8] J. Kovacs-Nolan, M. Phillips, Y. Mine, Advances in the value of eggs and egg components for human health, J. Agric. Food. Chem. 53 (2005) 8421–8431.

[9] S. Wang, M. Wei, Y. Huang, Biosorption of multifold toxic heavy metal ions from aqueous water onto food residue eggshell membrane functionalized with ammonium thioglycolate, J. Agric. Food. Chem. 61 (2013) 4988–4996.

[10] M. Ahmad, A.R.A. Usman, S.S. Lee, S.-C. Kim, J.-H. Joo, J.E. Yang, Y.S. Ok, Eggshell and coral wastes as low cost sorbents for the removal of Pb^{2+}, Cd^{2+} and Cu^{2+} from aqueous solutions, J. Ind. Eng. Chem. 18 (2012) 198–204.

[11] B. Liu, Y. Huang, Polyethyleneimine modified eggshell membrane as a novel biosorbent for adsorption and detoxification of Cr(VI) from water, J. Mater. Chem. 21 (2011) 17413–17418.

[12] P.S. Guru, S. Dash, Adsorption of some tailor-made styrylpyridinium dyes on sodium dodecylsulphate-treated eggshell particles (SDS-ESP): Impact of dye chain-length and substituent, J. Dispersion Sci. Technol. 34 (2013) 898–907.

[13] P.S. Guru, S. Dash, Eggshell particles (ESP) as potential adsorbent for styryl pyridinium dyes—A kinetic and thermodynamic study, J. Dispersion Sci. Technol. 33 (2012) 1012–1020.

[14] B. Koumanova, P. Peeva, S.J. Allen, K.A. Gallagher, M.G. Healy, Biosorption from aqueous solutions by eggshell membranes and *Rhizopus oryzae*: Equilibrium and kinetic studies, J. Chem. Technol. Biotechnol. 77 (2002) 539–545.

[15] C.M. Futalan, C.C. Kan, M.L. Dalida, C. Pascua, M.W. Wan, Fixed-bed column studies on the removal of copper using chitosan immobilized on bentonite, Carbohydr. Polym. 83 (2011) 697–704.

[16] M. Rinaudo, Chitin and chitosan: Properties and applications, Prog. Polym. Sci. 31 (2006) 603–632.

[17] P.K. Dutta, J. Dutta, V.S. Tripathi, Chitin and chitosan: Chemistry, properties and applications, J. Sci. Ind. Res. 63 (2004) 20–31.

[18] D.-W. Cho, B.-H. Jeon, C.-M. Chon, Y. Kim, F.W. Schwartz, E.-S. Lee, H. Song, A novel chitosan/clay/magnetite composite for adsorption of Cu(II) and As(V), Chem. Eng. J. 200–202 (2012) 654–662.

[19] M.R. Gandhi, G.N. Kousalya, S. Meenakshi, Selective sorption of Fe(III) using modified forms of chitosan beads, J. Appl. Polym. Sci. 124 (2011) 1858–1865.

[20] A.H. Chen, S.C. Liu, C.Y. Chen, C.Y. Chen, Comparative adsorption of Cu(II), Zn(II), and Pb(II) ions in aqueous solution on the crosslinked chitosan with epichlorohydrin, J. Hazard. Mater. 154 (2008) 184–191.

[21] M.B. Veera, A. Krishnaiah, J.R. Ann, D.S. Edgar, Removal of copper (II) and nickel (II) ions from aqueous solutions by a composite chitosan biosorbent, Sep. Sci. Technol. 43 (2008) 1365–1381.

[22] W.S. Wan Ngah, C.S. Endud, R. Mayanar, Removal of copper(II) ions from aqueous solution onto chitosan and cross-linked chitosan beads, React. Funct. Polym. 50 (2002) 181–190.

[23] G. Ji, W. Bao, G. Gao, B. An, H. Zou, S. Gan, Removal of Cu (II) from aqueous solution using a novel crosslinked alumina-chitosan hybrid adsorbent, Chin. J. Chem. Eng. 20 (2012) 641–648.

[24] C.M. Futalan, C.-C. Kan, M.L. Dalida, C. Pascua, K.-J. Hsien, M.-W. Wan, Copper, nickel and lead adsorption from aqueous solution using chitosan-immobilized on bentonite in a ternary system, Sustain. Environ. Res. 22 (2012) 345–355.

[25] C.M. Futalan, C.C. Kan, M.L. Dalida, K.J. Hsien, C. Pascua, M.W. Wan, Comparative and competitive adsorption of copper, lead, and nickel using chitosan immobilized on bentonite, Carbohydr. Polym. 83 (2011) 528–536.

[26] C.M. Futalan, C.C. Kan, M.L. Dalida, C. Pascua, K.J. Hsien, M.W. Wan, Nickel removal from aqueous solution in fixed bed using chitosan coated bentonite, Sustain. Environ. Res. 21 (2011) 361–367.

[27] J.Q. Albarelli, M.T. Luna, R.S. Vieira, M.M. Beppu, Evaluation of glass beads coated with chitosan for the adsorption of copper(II) ions from aqueous solution, Adsorpt. Sci. Technol. 30 (2012) 227–240.

[28] Y. Vijaya, M. Venkata Subbaiah, A. Subba Reddy, A. Krishnaiah, Equilibrium and kinetic studies of fluoride adsorption by chitosan coated perlite, Desalin. Water Treat. 20 (2010) 272–280.

[29] K. Swayampakula, V.M. Boddu, S.K. Nadavala, K. Abburi, Competitive adsorption of Cu(II), Co(II) and Ni (II) from their binary and tertiary aqueous solutions using chitosan-coated perlite beads as biosorbent, J. Hazard. Mater. 170 (2009) 680–689.

[30] S. Hasan, T.K. Ghosh, D.S. Viswanath, V.M. Boddu, Dispersion of chitosan on perlite for enhancement of copper(II) adsorption capacity, J. Hazard. Mater. 152 (2008) 826–837.

[31] S. Kalyani, J.A. Priya, P.S. Rao, A. Krishnaiah, Removal of copper and nickel from aqueous solutions using chitosan coated on perlite as biosorbent, Sep. Sci. Technol. 40 (2005) 1483–1495.

[32] S.R. Popuri, Y. Vijaya, V.M. Boddu, K. Abburi, Adsorptive removal of copper and nickel ions from water using chitosan coated PVC beads, Bioresour. Technol. 100 (2009) 194–199.

[33] M.W. Wan, C.C. Kan, C.H. Lin, D.R. Buenda, C.H. Wu, Adsorption of copper (II) by chitosan immobilized on sand, Chia-Nan Annu. Bull. 33 (2007) 96–106.

[34] M.W. Wan, I.G. Petrisor, H.T. Lai, D. Kim, T.F. Yen, Copper adsorption through chitosan immobilized on sand to demonstrate the feasibility for *in situ* soil decontamination, Carbohydr. Polym. 55 (2004) 249–254.

[35] W.T. Tsai, J.M. Yang, C.W. Lai, Y.H. Cheng, C.C. Lin, C.W. Yeh, Characterization and adsorption properties of eggshells and eggshell membrane, Bioresour. Technol. 97 (2006) 488–493.

[36] G. Busca, C. Resini, Vibrational spectroscopy for the analysis of geological and inorganic materials, in: R.A. Meyers (Ed.), Encyclopedia of Analytical Chemistry, John Wiley & Sons, Chichester, 2000, pp. 10954–11008.

[37] M. Ray, K. Pal, A. Anis, A.K. Banthia, Development and characterization of chitosan-based polymeric hydrogel membranes, Des. Monomers Polym. 13 (2010) 193–206.

[38] D. Enescu, V. Hamciuc, L. Pricop, T. Hamaide, V. Harabagiu, B.C. Simionescu, Polydimethylsiloxane-modified chitosan I. Synthesis and structural characterisation of graft and crosslinked copolymers, J. Polym. Res. 16 (2009) 73–80.

[39] W.S. Wan Ngah, L.C. Teong, R.H. Toh, M.A.K.M. Hanafiah, Comparative study on adsorption and desorption of Cu(II) ions by three types of chitosan-zeolite composites, Chem. Eng. J. 223 (2013) 231–238.

[40] P.H. Jai, J.S. Wook, Y.J. Kyu, K.B. Gil, L.S. Mok, Removal of heavy metals using waste eggshell, J. Environ. Sci. 19 (2007) 1436–1441.

[41] H.A. Aziz, M.N. Adlan, K.S. Ariffin, Heavy metals (Cd, Pb, Zn, Ni, Cu and Cr(III)) removal from water in Malaysia: Post treatment by high quality limestone, Bioresour. Technol. 99 (2008) 1578–1583.

[42] W.S.W. Wan Ngah, A. Kamari, Y.J. Koay, Equilibrium and kinetics studies of adsorption of copper (II) on chitosan and chitosan/PVA beads, Int. J. Biol. Macromol. 34 (2004) 155–161.

[43] F.C. Wu, R.L. Tseng, R.S. Juang, Kinetic modeling of liquid-phase adsorption of reactive dyes and metal ions on chitosan, Water Res. 35 (2001) 613–618.

[44] V.M. Boddu, K. Abburi, J.L. Talbott, E.D. Smith, Removal of hexavalent chromium from wastewater using a new composite chitosan biosorbent, Environ. Sci. Technol. 37 (2003) 4449–4456.

[45] M.K. Sureshkumar, D. Das, M.B. Mallia, P.C. Gupta, Adsorption of uranium from aqueous solution using chitosan-tripolyphosphate (CTPP) beads, J. Hazard. Mater. 184 (2010) 65–72.

[46] M. Del Bubba, C.A. Arias, H. Brix, Phosphorus adsorption maximum of sands for use as media in subsurface flow constructed reed beds as measured by the Langmuir isotherm, Water Res. 37 (2003) 3390–3400.

[47] D.W. Cho, C.M. Chon, Y. Kim, B.H. Jeon, F.W. Schwartz, E.S. Lee, H. Song, Adsorption of nitrate and Cr(VI) by cationic polymer-modified granular activated carbon, Chem. Eng. J. 175 (2011) 298–305.

[48] D. Das, M.K. Sureshkumar, K. Radhakrishnan, J. Nuwar, C.G.S. Pillai, Adsorptive removal of Cr(III) from aqueous solution using tripolyphosphate cross-linked chitosan beads, J. Radioanal. Nucl. Chem. Art. 289 (2011) 275–285.

[49] P. Sampranpiboon, P. Charnkeitkong, X. Feng, Equilibrium isotherm models for adsorption of zinc (II) ion from aqueous solution on pulp waste, WSEAS Trans. Environ. Dev. 10 (2014) 35–47.

[50] D.J.D. Dina, A.R. Ntieche, J.N. Ndi, J. Ketcha Mbadcam, Adsorption of acetic acid onto activated carbons obtained from maize cobs by chemical activation with zinc chloride ($ZnCl_2$), Res. J. Chem. Sci. 2 (2012) 42–49.

[51] Y.S. Al-Degs, M.I. El-Barghouthi, A.H. El-Sheikh, G.M. Walker, Effect of solution pH, ionic strength, and temperature on adsorption behavior of reactive dyes on activated carbon, Dyes Pigm. 77 (2008) 16–23.

[52] K.H. Chu, Removal of copper from aqueous solution by chitosan in prawn shell: Adsorption equilibrium and kinetics, J. Hazard. Mater. 90 (2002) 77–95.

[53] L. Jin, R. Bai, Mechanisms of lead adsorption on Chitosan/PVA hydrogel beads, Langmuir 18 (2002) 9765–9770.

[54] S.Y. Quek, D.A.J. Ise, C.P. Forster, The use of sago waste for the sorption of lead and copper, Water SA 24 (1998) 251–256.

[55] A. Kamari, W.S.W. Ngah, Isotherm, kinetic and thermodynamic studies of lead and copper uptake by H_2SO_4 modified chitosan, Colloids Surf., B 73 (2009) 257–266.

[56] R. Kobiraj, U. Nadeem, M.C. Chattopadhyaya, Removal of copper from aqueous solution using eggshell as an adsorbent, J. Ind. Chem. Soc. 88 (2011) 819–825.